



141
153
THS

**LIBRARY
Michigan State
University**

This is to certify that the
dissertation entitled

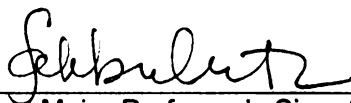
**HEEGAARD FLOER HOMOLOGY OF CERTAIN
3-MANIFOLDS AND COBORDISM INVARIANTS**

presented by

Daniel Selahi Durusoy

has been accepted towards fulfillment
of the requirements for the

Ph.D. degree in Mathematics



Major Professor's Signature

April 16 / 08

Date

PLACE IN RETURN BOX to remove this checkout from your record.
TO AVOID FINES return on or before date due.
MAY BE RECALLED with earlier due date if requested.

DATE DUE	DATE DUE	DATE DUE

HEEGAARD FLOER HOMOLOGY OF CERTAIN 3-MANIFOLDS
AND COBORDISM INVARIANTS

By

Daniel Selahi Durusoy

A DISSERTATION

Submitted to
Michigan State University
in partial fulfillment of the requirements
for the degree of

DOCTOR OF PHILOSOPHY

Mathematics

2008

ABSTRACT

HEEGAARD FLOER HOMOLOGY OF CERTAIN 3-MANIFOLDS AND COBORDISM INVARIANTS

By

Daniel Selahi Durusoy

In this thesis, we study the Heegaard Floer homology of 3-manifolds which is introduced by Peter Ozsváth and Zoltan Szabó. We first look at certain Brieskorn homology spheres. We then consider the question of which 3-manifolds bound rational homology 4-balls, and give partial answer in the case of Brieskorn homology spheres $\Sigma(p, q, r)$ with small values for p, q, r using the obstruction d defined through cobordism maps between Heegaard Floer homologies.

To my parents

Acknowledgments

I would like to thank my advisor, Dr. Selman Akbulut for his excellent guidance, help and encouragement throughout all of my study at Michigan State University.

Many thanks to the members of my advisory committee Dr. Ronald Fintushel, Dr. Nikolai Ivanov, Dr. Lawrence Roberts and Dr. Michael Shapiro. I would also like to thank my friends and fellow graduate students, in particular, Svetlana Roudenko, Onur Agirseven, Jens von Bergmann, Firat Arikan, Jim Carter, Steve Miller, Susanne Kleff, Don and Becky McMahon for useful discussions and keeping me motivated.

Finally, I would like to thank Dr. Sergey Finashin, Dr. Mustafa Korkmaz, Dr. Yildiray Ozan and Dr. Turgut Önder from Middle East Technical University who have introduced me to the field of geometric topology.

Table of Contents

List of Tables	vi
List of Figures	vii
1 Introduction	1
2 Background on Heegaard Floer homology	3
2.1 Heegaard diagrams	3
2.2 Symmetric product and the chain complex	9
2.3 L-spaces	15
2.4 Absolute gradings	15
3 Floer homology of certain 3-manifolds	17
3.1 Plumbing diagrams	17
3.2 Floer homology of certain homology spheres	19
3.3 A combinatorial model	19
3.4 Floer homology of $\Sigma(2, 5, 7)$	22
3.5 The family $\Sigma(2, 3, 6n + 1)$	24
4 Invariants of cobordisms	28
4.1 d -invariant	28
5 Action of diffeomorphisms	33
5.1 An involution	33
A Appendix: Plumbing graphs	35
Bibliography	40

List of Tables

4.1	Values of d and $\bar{\mu}$ for $r \leq 11$	31
4.2	List of Brieskorn spheres with $d = 0$ with $r \leq 13$	32
A.1	Plumbing graphs for $\Sigma(p, q, r)$ with $d = 0$ and $r \leq 13$	35

List of Figures

2.1	$T^3 = nd(\Gamma) \cup nd(\Gamma')$	4
2.2	Standard system of curves on ∂H_g	6
2.3	A Heegaard diagram for S^3	7
2.4	Sliding β_2 over β_1	8
2.5	Destabilizing a Heegaard diagram	8
2.6	Pointed Heegaard diagrams for S^3 and $S^1 \times S^2$	9
2.7	Whitney disk representing an element of $\pi_2(x, y)$	10
2.8	Whitney triangle representing an element of $\pi_2(x, y, z)$	12
2.9	Heegaard triples	13
2.10	Three views for the standard genus 1 Heegaard diagram for S^3	14
2.11	Three views for the standard genus 1 Heegaard diagram for $S^1 \times S^2$.	14
3.1	Rational surgery description of $\Sigma(a_1, a_2, a_3)$	17
3.2	Plumbing graph for $\Sigma(2, 5, 7)$	22
3.3	Equivalences in $K^+(G)$	23
5.1	$Z_{id} = X \cup -X$ and $Z_f = X \cup_f -X$	33

Chapter 1

Introduction

Floer homology was introduced by Andreas Floer [F11, F12] which was built on the ideas of Morse theory of critical points. Since then several homology theories have been defined using the same basic principles, the so called Floer-type homologies. Starting in 2001, Peter Ozsváth and Zoltan Szabó [OS1] have defined and extended Heegaard Floer homology for 3 and 4 manifolds, and eventually for knots in 3-manifolds, whose setup is similar to the Lagrangian intersection Floer homology. The generators of the chain group are intersections of two Lagrangians which are the products of Heegaard curves, inside the symmetric product of the Heegaard surface [OS1, Pe] and the boundary map counts holomorphic disks connecting the intersection points.

Heegaard Floer homology is well suited for calculations and has provided new proofs of famous results such as the following: symplectic 4-manifolds have non-trivial invariant, Milnor conjecture for torus knots, and recently it has been used in finishing the proof of the Property P conjecture. Also, the version for knots can detect the genus of a knot, and also fiberedness of a knot.

This new setup is also based on gauge theory, but recently it has been shown to admit

some purely combinatorial descriptions, too. One of them [SW] is based on modifying a given Heegaard diagram so that it will have only simple regions except one, which is enough to recover hat theory combinatorially, and the other one is based on starting with a grid diagram for a link [MO1, MO2] which gives a simple Heegaard diagram to start with, but probably of very high genus. In both versions number of generators tend to be very large, but in many cases the homology groups can be computed using a computer.

In this thesis we use the combinatorial approach given by Ozsváth and Szabó [OS4] to compute HF^+ for negative definite plumbings with at most one bad vertex. In particular, we use these techniques to compute

Theorem 1.1. $HF^+(-\Sigma(2, 5, 7)) = T_0^+ \oplus \mathbb{Z}_{(0)}^2$.

Theorem 1.2. $HF^+(-\Sigma(2, 3, 6n + 1)) = T_0^+ \oplus \mathbb{Z}_{(0)}^n$.

The Brieskorn spheres in Theorem 1.2 are obtained as $-1/n$ surgery on the right handed trefoil knot also as $+1$ surgery on the twist knot with $2n + 2$ crossings. In [OS3] Ozsváth and Szabó have computed $HF^+(\Sigma(2, 3, 6n + 1))$ (denoted by $Z_{-1/n}$ in that paper) using surgery exact sequence and that $+5$ surgery on the trefoil is a lens space. By reversing orientation we show that we get the same result.

We also investigate values of the d invariant, which is an invariant of $spin^c$ rational homology cobordism. In particular, for integral homology spheres it gives an obstruction to bounding rational homology 4-balls.

Recently Lisca [Li] has applied the celebrated theorem of Donaldson to list all lens spaces that smoothly bound rational homology 4-balls. We investigate the intersection forms for the canonical negative definite 4-manifolds bounding Brieskorn spheres and provide a list of results.

Chapter 2

Background on Heegaard Floer homology

2.1 Heegaard diagrams

We will be working with smooth closed oriented 3-manifolds, unless stated otherwise.

A **solid handlebody** of genus g is the compact 3-manifold homeomorphic to a tubular neighborhood of a wedge of g circles in \mathbb{R}^3 . The boundary of a solid handlebody H_g is the closed surface of genus g , which we denote by Σ_g .

Definition 2.1. A **Heegaard splitting** of Y^3 is a decomposition of Y into a union of two solid handlebodies along their common boundary:

$$Y = H_\alpha \cup_{\Sigma_g} H_\beta,$$

for some $g \geq 0$.

The embedding of H_α and H_β into Y induces a gluing map $\phi : \partial H_\alpha \longrightarrow \partial H_\beta$ on their common boundary Σ_g up to conjugation by an element of the mapping class group.

Proposition 2.2. *Each closed connected 3-manifold Y admits a Heegaard splitting.*

Proof. We recall the sketch of proof from [Ro], page 240. The main ingredient is the fact that each 3-manifold is triangulable. Let H be the tubular neighbourhood of the 1-skeleton of a triangulation. Then its complement is also the tubular neighbourhood of a 1-complex (the dual 1-complex), which is also a solid handlebody. \square

Example 2.3. We describe a Heegaard splitting of the 3-torus T^3 . Consider the graph Γ in T^3 where we visualize T^3 as the quotient of the cube obtained by gluing the opposite faces together via translation. Since Γ is a connected graph, its tubular neighborhood is a solid handlebody. Note that its complement is the tubular neighborhood of the graph Γ' obtained by the image of the edges of the cube in the quotient, hence we get a genus 3 splitting of T^3 .

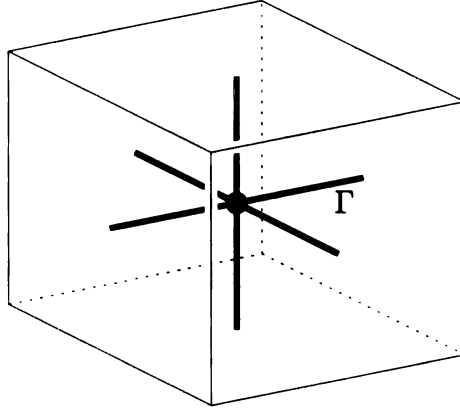


Figure 2.1: $T^3 = nd(\Gamma) \cup nd(\Gamma')$.

A Heegaard splitting can be encoded by a pair of sets of curves on the Heegaard surface Σ_g . These curves will be the boundaries of a set of compression disks for the solid handlebodies H_α, H_β , which cut the corresponding solid handlebody into B^3 .

Definition 2.4. A **Heegaard diagram** of a 3-manifold Y is a triple $(\Sigma_g, \alpha, \beta)$ where Σ_g is a Heegaard surface and α and β are sets of pairwise disjoint g simple closed curves on Σ_g that cut Σ_g into punctured S^2 .

Remark 2.5. The curves $\alpha_1, \dots, \alpha_g$ are essential curves and their homology classes are linearly independent in $H_1(\Sigma_g)$. We will call such set of curves a **system of curves**. They are maximal in the sense that any other curve disjoint from given ones has to be linearly dependent. Same statement is true for β curves. In fact, switching the α and β curves corresponds to changing the orientation of the 3-manifold.

To recover a 3-manifold Y^3 from a given Heegaard diagram, we look at $\Sigma_g \times I$ and add 2-handles along $(\alpha, 0)$ and also 2-handles along $(\beta, 1)$. Since α and β are systems of curves, this 3-manifold has boundary $S^2 \amalg S^2$, and we cap these off by gluing copies of B^3 .

It is instructional to look at the same concept from the Morse theoretic point of view. Given a self indexing Morse function $f : Y^3 \rightarrow \mathbb{R}$, with only one index 0 and one index 3 critical point, we obtain a Heegaard splitting by taking $H_\alpha = f^{-1}\left(\left[0, \frac{3}{2}\right]\right)$ and $H_\beta = f^{-1}\left(\left[\frac{3}{2}, 3\right]\right)$. Since the Morse function gives a handle decomposition for Y^3 , H_α will be precisely the union of the unique 0-handle and the g 1-handles, which is a solid handlebody. We see that H_β , the complement of H_α , is also a solid handlebody by turning Y^3 upside down, i.e. $f \mapsto -f$. The compression disks will correspond to the ascending and descending disks at the index 1 and 2 critical points of f , respectively.

Proposition 2.6. *After a homeomorphism of the surface, we can always take the α curves to be the standard system of curves for the model solid handlebody H_g as in figure 2.2.*

Proof. Given a Heegaard diagram $(\Sigma_g, \alpha, \beta)$, cutting Σ_g along α gives a sphere with $2g$ holes. The same is true with the α curves given in Figure 2.2. This gives us a homeomorphism from $\Sigma_g \setminus \alpha$ to $(\partial H_g) \setminus \alpha$. Now observe that this homeomorphism

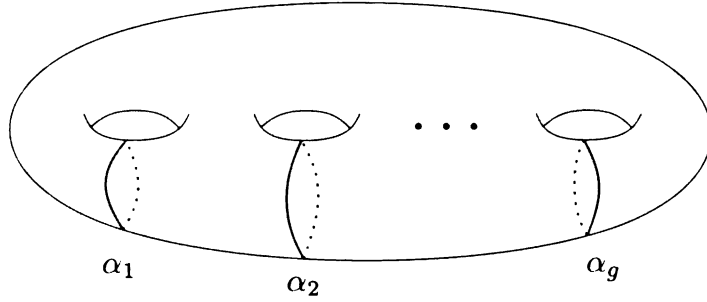


Figure 2.2: Standard system of curves on ∂H_g

extends to the closed surface. □

Due to this proposition, any Heegaard diagram can be drawn with only β curves on the model solid handlebody. Even though not drawing α curves might seem useful at first, it doesn't fit our purposes since we will need to see where the α and β curves intersect.

Remark 2.7. The information carried in a Heegaard diagram is how H_α is glued to H_β , which can be considered as an element ϕ of the mapping class group of the Heegaard surface after identifying ∂H_α with a standard genus g handlebody. For a different identification, we get conjugates of ϕ . Composing ϕ with an element of the Torelli group gives the same 3-manifold.

Example 2.8 (A Heegaard diagram for S^3). In Figure 2.3, we see Σ_2 and two pairs of curves on it (adapted from [Ro], page 243). Since α_1 and α_2 are linearly independent, and similarly β_1 and β_2 , this gives a Heegaard diagram.

We can cut along α_1 and α_2 to get 4 times punctured S^2 , hence we can represent the Heegaard diagram as a planar diagram as shown in the middle of Figure 2.3. Now it becomes obvious that we can slide the feet of the 1-handles to obtain the obvious Heegaard diagram for $S^3 \# S^3$ where we see two cancelling pairs.

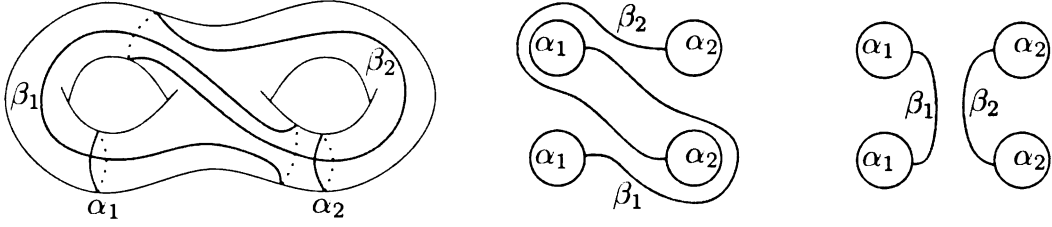


Figure 2.3: A Heegaard diagram for S^3

Example 2.9. The only 3-manifolds which admit genus 1 Heegaard splittings are the Lens spaces $L(p, q)$. In particular $L(p, 0) = S^3$ and $L(0, q) = S^1 \times S^2$. Their Heegaard diagrams have α_1 representing $(0, 1)$ and β_1 representing $(-p, q)$ on the torus.

The Reidemester-Singer theorem tells that any two Heegaard diagrams of Y^3 are stably isotopic. This can be formulated as follows:

Theorem 2.10. *Any two Heegaard diagrams for Y can be connected by a sequence of the following moves:*

1. *isotopies of α and β , through one parameter family of systems of curves,*
2. *handle slides among α and handle slides among β ,*
3. *stabilization and destabilization.*

For the proof, we refer the reader to Proposition 2.2 in [OS1].

A **handle slide** among α curves means isotoping one of the attaching circles α_i over the core disk in H_α of another α_j . This is illustrated in Figure 2.4. As a final step we can isotope β'_2 and get a completely symmetric diagram, which corresponds to the 3-manifold $(S^1 \times S^2) \# (S^1 \times S^2)$.

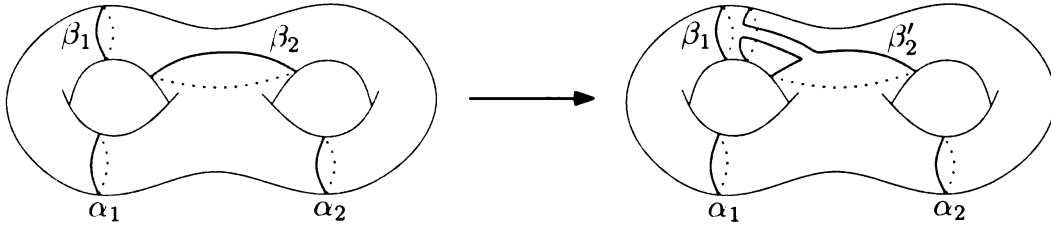


Figure 2.4: Sliding β_2 over β_1

Stabilization is the process of taking the connected sum of the Heegaard surface with a torus containing curves $\alpha_{g+1}, \beta_{g+1}$ lying as the standard longitude-meridian pair. In terms of the 3-manifold this corresponds to a connected sum with S^3 .

Destabilization is the inverse operation, namely if only β_g intersects α_g , and geometrically once, then the diagram can be simplified by compressing Σ_g along the disk that α_g bounds in H_α and erasing β_g from the diagram, see Figure 2.5.

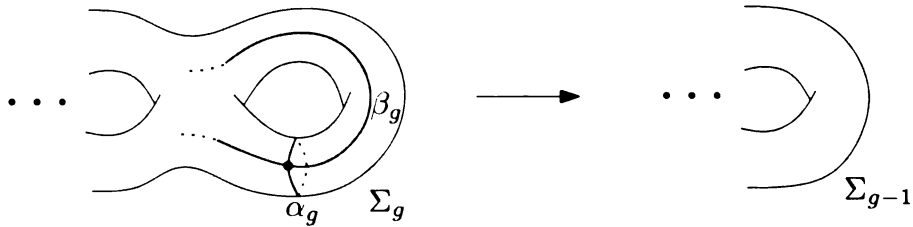


Figure 2.5: Destabilizing a Heegaard diagram

For the purposes of Heegaard Floer homology, we will need marked Heegaard diagrams. Marking a point on Σ_g avoiding α and β gives rise to a choice of $spin^c$ structure on Y^3 for each generator. Furthermore two distinct points on a Heegaard diagram encode a knot in Y^3 as follows: given a Heegaard diagram compatible with a Morse function f with a unique maximum and a unique minimum and two points $z, w \in \Sigma_g - (\alpha \cup \beta)$, consider the flow-lines connecting index 0 and index 3 critical points to z and w . These four arcs make up an oriented closed embedded curve in Y^3 (start traveling at the maximum, visit z first).

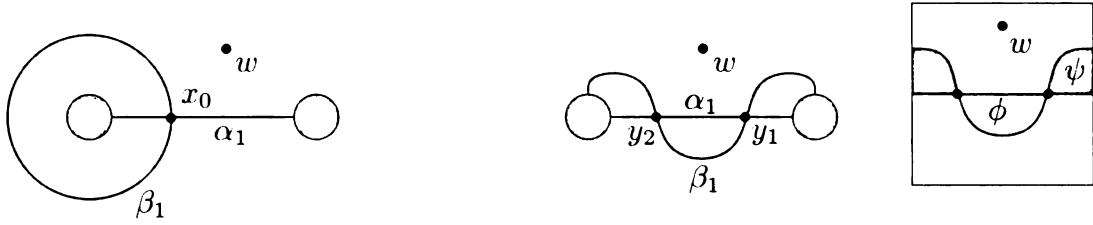


Figure 2.6: Pointed Heegaard diagrams for S^3 and $S^1 \times S^2$

2.2 Symmetric product and the chain complex

Heegaard Floer homology is inspired by Lagrangian intersection Floer homology introduced by Andreas Floer in [Fl1]. The symplectic manifold that is used in Heegaard Floer homology is the symmetric product of the Heegaard surface, and the generators for the chain complex will be the intersections of two totally real tori in the symmetric product.

Definition 2.11. The k^{th} **symmetric product** of a surface Σ_g is the quotient of the product $\Sigma_g \times \cdots \times \Sigma_g$ (k factors) under the action of the symmetric group on k letters. It is denoted by $Sym^k \Sigma_g$.

A point $\mathbf{x} \in Sym^k \Sigma_g$ means unordered k points $\{x_1, \dots, x_k\}$ (not necessarily distinct) on Σ_g . Unless mentioned otherwise, we will use $k = g$. In particular we will denote $Sym^g \Sigma_g$ by $\Sigma^{(g)}$. Note that the symmetric product of a surface is a $2k$ -dimensional manifold, whereas in general symmetric products of manifolds of other dimensions have orbifold singularities.

The curves α and β define g -dimensional tori in $\Sigma^{(g)}$ as follows: let \mathbb{T}_α be the set of points \mathbf{x} with $x_i \in \alpha_i$ for $1 \leq i \leq g$. This is indeed an imbedded g -dimensional torus since the curves α_i are disjoint. Similarly we have the torus \mathbb{T}_β .

2.2.1 Holomorphic disks

The chain groups $\widehat{CF}(Y)$ are freely generated by intersection points of \mathbb{T}_α and \mathbb{T}_β . Similarly The chain groups $CF^\infty(Y)$ are generated by $[x, i]$ for $x \in \mathbb{T}_\alpha \cap \mathbb{T}_\beta$ and $i \in \mathbb{Z}$. The boundary operator is defined via counting holomorphic Whitney disks:

Definition 2.12. A **Whitney disk** u between $x, y \in \mathbb{T}_\alpha \cap \mathbb{T}_\beta$ is a continuous map $u : \mathbb{D} \longrightarrow \Sigma^{(g)}$ with $u(\{0\} \times \mathbb{R}) \subset \mathbb{T}_\beta$, $u(\{1\} \times \mathbb{R}) \subset \mathbb{T}_\alpha$, $\lim_{t \rightarrow -\infty} u(s, t) = x$ and $\lim_{t \rightarrow \infty} u(s, t) = y$. The set of homotopy classes of Whitney disks from x to y is denoted by $\pi_2(x, y)$.

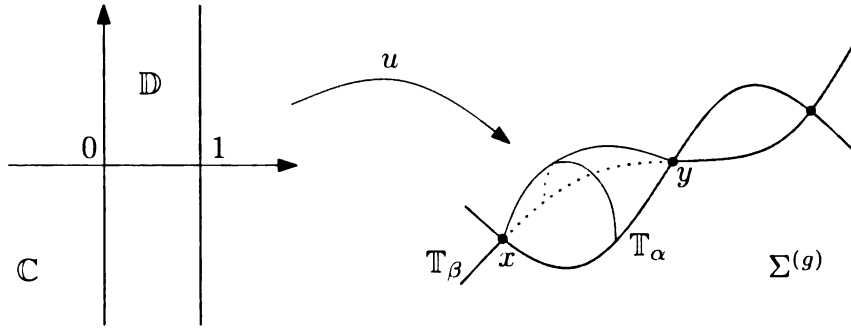


Figure 2.7: Whitney disk representing an element of $\pi_2(x, y)$

Let $\phi \in \pi_2(x, y)$. The local multiplicity $n_w(\phi)$ of ϕ is defined to be the algebraic intersection number of $\phi(\mathbb{D})$ with $\{u\} \times \text{Sym}^{g-1}\Sigma$.

The set of holomorphic disks which represent ϕ is the moduli space $\mathcal{M}(\phi)$, and its dimension is the Maslov index, denoted by $\mu(\phi)$. There is an action of \mathbb{R} on $\mathcal{M}(\phi)$ given by precomposing u with a vertical translation in \mathbb{D} . We will denote the quotient $\mathcal{M}(\phi)/\mathbb{R}$ by $\widehat{\mathcal{M}}(\phi)$.

Proposition 2.13. *If ϕ has a holomorphic representative u , then $n_w(\phi) \geq 0$.*

Proof. Because of the almost complex structures chosen, $\{w\} \times \Sigma^{(g-1)}$ is a holomorphic variety and the intersection of two holomorphic varieties is non-negative. \square

Remark 2.14. If $n_w(\phi) < 0$ then $\mathcal{M}(\phi)$ is empty.

Proposition 2.15 ([OS1], Prop 2.15). *When $g > 1$, if $\pi_2(x, y) \neq \emptyset$ then*

$$\pi_2(x, y) \cong \mathbb{Z} \oplus H^1(Y; \mathbb{Z}).$$

The boundary operator is defined by $\partial[x, i] = \sum_{\phi \in \pi_2(x, y), \mu(\phi)=1} \# \widehat{\mathcal{M}}(\phi) \cdot [y, i - n_w(\phi)]$.

Recall figure 2.6 given in page 9. From the Heegaard diagram we see that $\widehat{CF}(S^3)$ is generated by a single element. For $S^1 \times S^2$ there are two generators y_1 and y_2 . In general when $b_1(Y) > 0$ a special class of Heegaard diagrams are used so that the resulting homology is an invariant. Note that in that figure β_1 could be isotoped to get rid of the intersection points, and that would mean there would be no generators for the Floer homology. But that is not an admissible Heegaard diagram in the sense of [OS1]. We will revisit these examples in section 2.2.4.

2.2.2 Heegaard Floer chain complex

There is a \mathbb{Z} action on $CF^\infty(Y)$ given by $U[x, i] = [x, i - 1]$. By definition it decreases the homological grading by 2. The subcomplex generated by $[x, i]$ for $i < 0$ is called $CF^-(Y)$. The inclusion $CF^-(Y) \subset CF^\infty(Y)$ fits into the following short exact sequence of chain complexes, where $CF^+(Y)$ is the quotient complex:

$$0 \longrightarrow CF^-(Y) \longrightarrow CF^\infty(Y) \longrightarrow CF^+(Y) \longrightarrow 0$$

On the other hand the U map has a kernel which we call $\widehat{CF}(Y)$:

$$0 \longrightarrow \widehat{CF}(Y) \longrightarrow CF^+(Y) \xrightarrow{U} CF^+(Y) \longrightarrow 0$$

These short exact sequences induce the following long exact sequences in homology:

$$\dots \longrightarrow HF^-(Y) \xrightarrow{\iota} HF^\infty(Y) \xrightarrow{\pi} HF^+(Y) \xrightarrow{\delta} \dots \quad (2.1)$$

$$\dots \longrightarrow \widehat{HF}(Y) \xrightarrow{\hat{\iota}} HF^+(Y) \xrightarrow{U} HF^+(Y) \xrightarrow{\delta} \dots \quad (2.2)$$

All these chain groups can be obtained from $CF^-(Y)$ as follows:

- CF^∞ is the localization $CF^-(Y) \otimes \mathbb{Z}[U, U^{-1}]$,
- $CF^+(Y)$ is the cokernel of the localization map,
- $\widehat{CF}(Y)$ is the quotient $CF^-(Y)/U \cdot CF^-(Y)$.

2.2.3 Holomorphic triangles

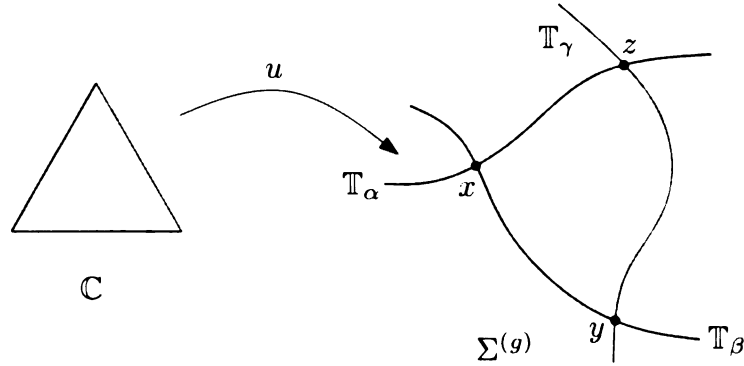


Figure 2.8: Whitney triangle representing an element of $\pi_2(x, y, z)$

Counting holomorphic triangles gives rise to a chain map

$$F_{\alpha, \beta, \gamma} : \widehat{CF}(Y_{\alpha\beta}, t_{\alpha\beta}) \otimes \widehat{CF}(Y_{\beta\gamma}, t_{\beta\gamma}) \longrightarrow \widehat{CF}(Y_{\alpha\gamma}, t_{\alpha\gamma})$$

$$x \otimes y \mapsto \sum_{\substack{\phi \in \pi_2(x, y, z), \mu(\phi)=0, \\ s_{u'}(\phi)=s, n_{u'}(\phi)=0}} \# \mathcal{M}(\phi) \cdot z.$$

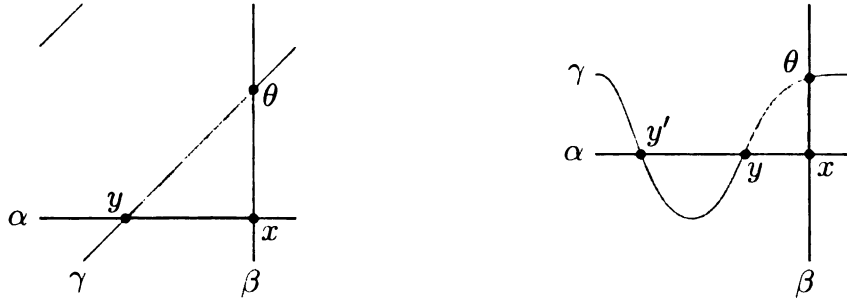


Figure 2.9: Heegaard triples

In figure 2.9 there is a small triangle $\psi \in \pi_2(x, \theta, y')$ but it is not orientation preserving, hence can't be holomorphic. Hence we have $F_W(x) = y$, and F_W increases absolute grading by $\frac{1}{2}$, hence $\tilde{gr}(y) = -\frac{1}{2}$, and there is a holomorphic disk from y' to y , hence $\tilde{gr}(y') = \frac{1}{2}$.

2.2.4 Two examples: S^3 and $S^1 \times S^2$

We quote the Heegaard Floer homology of two basic 3-manifolds that we will need in later sections. Since S^3 has a unique $spin^c$ structure, we will omit it from the notation.

Lemma 2.16. *The Heegaard Floer homology of S^3 is given by*

$$\begin{aligned} \widehat{HF}(S^3) &= \mathbb{Z} \\ HF_d^\infty(S^3) &= \begin{cases} \mathbb{Z}, & d \text{ even} \\ 0, & d \text{ odd} \end{cases} \\ HF_d^+(S^3) &= \begin{cases} \mathbb{Z}, & d \geq 0 \text{ and even} \\ 0, & \text{otherwise} \end{cases} \\ HF_{red}(S^3) &= 0 \end{aligned}$$

The chain groups $\widehat{CF}(S^3)$ are generated by the single intersection point x in figure 2.10, hence boundary map is trivial. The chain groups $CF^\infty(S^3)$ are generated by $[x, i]$ for $i \in \mathbb{Z}$, and U is an isomorphism decreasing grading by 2, hence we get

the mentioned homology groups. $U : HF^+(S^3) \longrightarrow HF^+(S^3)$ is surjective, hence $HF_{red}(S^3) = HF^+(S^3)/Im(U^k) = 0$ where k is any large positive integer.

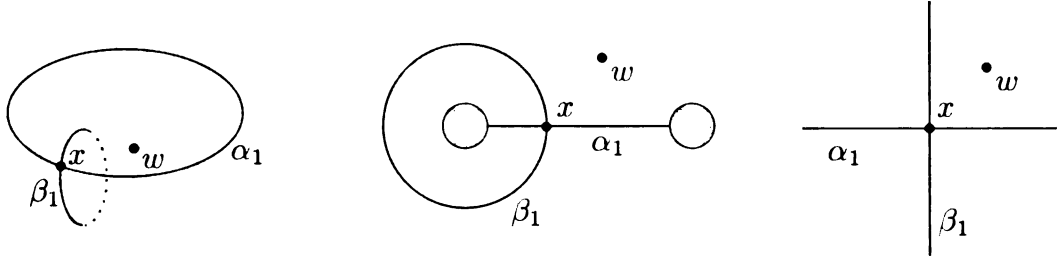


Figure 2.10: Three views for the standard genus 1 Heegaard diagram for S^3

Lemma 2.17. *The Heegaard Floer homology of $S^1 \times S^2$ is given by*

$$\begin{aligned} \widehat{HF}(S^1 \times S^2, t_0) &= \mathbb{Z}_{-\frac{1}{2}} \oplus \mathbb{Z}_{\frac{1}{2}} \\ HF_d^\infty(S^1 \times S^2, t_0) &= \begin{cases} \mathbb{Z}, & d \in \frac{1}{2} + \mathbb{Z} \\ 0, & \text{otherwise} \end{cases} \end{aligned}$$

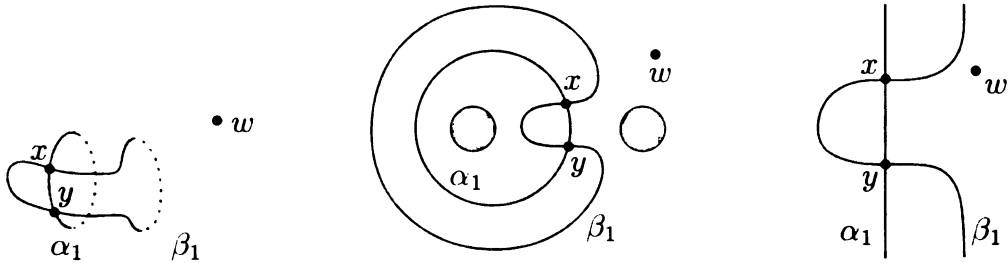


Figure 2.11: Three views for the standard genus 1 Heegaard diagram for $S^1 \times S^2$

There are two holomorphic disks connecting x to y with opposite signs, hence we get $\widehat{HF}(S^1 \times S^2) \cong \mathbb{Z} \oplus \mathbb{Z}$. The homological grading is initially defined as a relative grading, but in section 2.4 we tell how to obtain absolute gradings, and the rational gradings come from the degree shift formula.

2.3 L-spaces

Definition 2.18. A rational homology sphere Y is called an **L-space** if rank of $\widehat{HF}(Y)$ is same as the cardinality of $H_1(Y; \mathbb{Z})$.

Example 2.19. Lens spaces are L-spaces. If $S_n^3(K)$ is an L-space with $n > 0$, then $S_{n+1}^3(K)$ is also an L-space. The Poincaré homology sphere $\Sigma(2, 3, 5)$ is an L-space. Plumbed 3-manifolds with no bad vertices are L-spaces. Also branched double covers of S^3 along non-split alternating links are L-spaces.

2.4 Absolute gradings

Ozsváth and Szabó ([OS2], theorem 7.1) have shown that there is a consistent way to extend the relative gradings on rational homology 3-spheres to an absolute \mathbb{Q} -grading.

Definition 2.20. Heegaard Floer homology groups of rational homology spheres carry an **absolute grading** $\tilde{gr} : HF^\circ(Y, t) \longrightarrow \mathbb{Q}$ characterized as follows:

1. (normalization) $\widehat{HF}(S^3)$ is supported in grading 0.
2. (lifting) \tilde{gr} lifts relative grading: $gr(\xi, \eta) = \tilde{gr}(\xi) - \tilde{gr}(\eta)$
3. (cobordisms) $\tilde{gr}(F_{W,s}(\xi)) - \tilde{gr}(\xi) = \frac{1}{4} (c_1(s)^2 - 2\chi(W) - 3\sigma(W))$ for a cobordism (W, s) between (Y_1, t_1) and (Y_2, t_2) with torsion $spin^c$ structures
4. the maps $\hat{\iota}$, ι and π in equations 2.1 and 2.2 (see page 12) preserve \tilde{gr} and δ decreases \tilde{gr} by 1.

More concretely, if L is a framed link so that $Y = S^3(L)$, and $W = W(L)$ is the

corresponding cobordism, then for $y \in \widehat{CF}(Y)$,

$$\tilde{gr}(y) = -\mu(\psi) + 2n_w(\psi) + \frac{1}{4} \left(c_1(s)^2 - 2\chi(W) - 3\sigma(W) \right).$$

There is a duality pairing between on Heegaard Floer chain groups given as follows [OS3]:

$$\langle [x, i], [y, j] \rangle = \begin{cases} 1 & x = y, j = -i - 1 \\ 0 & \text{otherwise} \end{cases}$$

When $c_1(t)$ is torsion, $\langle \cdot, \cdot \rangle$ induces an isomorphism $CF^+(Y, t) \longrightarrow CF_-(-Y, s)$, hence an isomorphism $HF_i^+(Y, t) \longrightarrow HF_-^{i-2}(-Y, t)$ given by $[x, i] \mapsto -[x, -i-1]^*$.

Chapter 3

Floer homology of certain 3-manifolds

3.1 Plumbing diagrams

A **weighted graph** is a graph with integer weights associated to its vertices. Given a weighted graph G , there is a corresponding smooth 4-manifold $X(G)$ obtained as follows: for each vertex form the D^2 bundles over S^2 with Euler number given by the weight, and corresponding to each edge, plumb the corresponding D^2 bundles (and corners are smoothed). The boundary of $X(G)$ is a 3-manifold which we will denote by $Y(G)$.

Consider the Seifert fibered homology spheres with 3 singular fibers: they are the Brieskorn homology spheres $\Sigma(a_1, a_2, a_3)$ for relatively prime positive integers a_i :

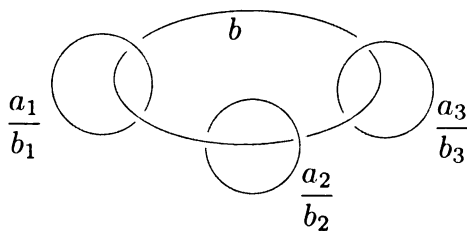


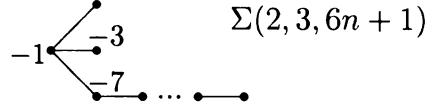
Figure 3.1: Rational surgery description of $\Sigma(a_1, a_2, a_3)$

Here, the unknowns are determined from the following equations:

$$a_1 \cdot a_2 \cdot a_3 \cdot \left(-b + \frac{b_1}{a_1} + \frac{b_2}{a_2} + \frac{b_3}{a_3} \right) = 1$$

where $b \leq -1$ and $b_i \leq -2$. These conditions determine a negative definite minimal plumbed 4-manifold with its boundary $\Sigma(a_1, a_2, a_3)$.

For example the following weighted graph G describes $Y(G) = \Sigma(2, 3, 6n + 1)$, where the total number of vertices is $n + 3$ and vertices where the weight is not written have weight -2 .



The intersection form on $H_2(X(G))$ is given by the adjacency matrix of the graph with the weights on the diagonal entries. For example, using the above graph with $n = 3$ we get the following intersection matrix:

$$\begin{bmatrix} -1 & 1 & 1 & 1 & 0 & 0 \\ 1 & -2 & 0 & 0 & 0 & 0 \\ 1 & 0 & -3 & 0 & 0 & 0 \\ 1 & 0 & 0 & -7 & 1 & 0 \\ 0 & 0 & 0 & 1 & -2 & 1 \\ 0 & 0 & 0 & 0 & 1 & -2 \end{bmatrix}$$

If this matrix is negative definite, the weighted graph is called negative definite.

Remark: The negative definite minimal plumbing diagram for $\Sigma(a_1, a_2, a_3)$ is characterized by

$$-a_i < b_i < -1 \quad \text{and} \quad b < 0.$$

Definition 3.1. A vertex v in a weighted graph G is called a **bad vertex** if $-v \cdot v < d(v)$ where $d(v)$ is the count of edges containing v .

According to this definition, all Brieskorn homology spheres $\Sigma(a_1, a_2, a_3)$ have a plumbing description with one bad vertex.

3.2 Floer homology of certain homology spheres

First we recall and explain the algorithm due to Ozsváth and Szabó [OS4] for computing HF^+ from certain plumbing diagrams.

Ozsváth and Szabó have given a combinatorial description for Heegaard-Floer homology in [OS4]. Using this algorithm we compute Heegaard-Floer homology of $-\Sigma(2, 3, 6n + 1)$:

Theorem 3.2. $HF^+(-\Sigma(2, 3, 6n + 1)) = T_0^+ \oplus \mathbb{Z}_{(0)}^n$.

This family of homology spheres can be obtained by doing $-1/n$ surgery on the right handed trefoil knot. This family and some more were considered in [FS3] where their instanton Floer homology is calculated. For the Heegaard-Floer homology computations for the family $\Sigma(2, 2n + 1, 4n + 3)$ see [Ru1]. Another combinatorial description for calculating HF^+ has been given by Némethi in [Ne].

3.3 A combinatorial model

In this section G will denote a negative definite weighted graph with at most one bad vertex. $X(G)$ is the plumbing 4-manifold and $Y(G) = \partial X(G)$, $W(G) = X(G) - B^4$ cobordism from $Y(G)$ to S^3 . Let $Char(G)$ denote the set of characteristic vectors in $H_2(X(G))$ with respect to the intersection form.

Given an element $\xi \in HF^+(-Y(G))$, we can define a map $\phi_\xi \in \text{Map}(\text{Char}(G), \mathcal{T}_0^+)$ by declaring $\phi_\xi(K) = F_{W(G), s_K}(\xi)$ where $c_1(s_K) = K$ and F_W is the map on Floer homology induced from the $Spin^c$ cobordism $(W(G), s_K)$.

Definition 3.3 ([OS4]). $\mathbb{H}^+(G) \subset \text{Map}(\text{Char}(G), \mathcal{T}_0^+)$ is the subset of finitely supported maps satisfying

$$U^{m+n} \cdot f(K + 2PD[v]) = U^m \cdot f(K) \quad \text{if} \quad \min\{m, m+n\} \geq 0 \text{ and } K \cdot v + v \cdot v = 2n$$

In [OS4] the following is shown:

Theorem 3.4 ([OS4], Thm 1.2). *For such a graph G , for each $Spin^c$ structure t over $-Y(G)$,*

$$HF^+(-Y(G), t) \cong \mathbb{H}^+(G, t).$$

We will be working with homology spheres, so we suppress the $Spin^c$ structure from the notation. In the computations instead of working with elements of $\mathbb{H}^+(G)$, [OS4] suggests working with elements of $K^+(G)$, which is the set of equivalence classes of elements in $\mathbb{Z}^{\geq 0} \times \text{Char}(G)$, with the equivalence relation defined by

$$(m, K) \sim (m+n, K + 2PD[v])$$

where v is a vertex in G with $K \cdot v + v \cdot v = 2n$ and $\min(m, m+n) \geq 0$. Equivalence class of (m, K) will be denoted by $U^m \otimes K$.

For an equivalence class $U^m \otimes K$, define its **U-depth** as the largest number l so that (l, K') is a representative of $U^m \otimes K$ for some vector K' . $K^+(G)$ is determined by elements of U -depth 0 and the U action on $K^+(G)$, which follows from

Proposition 3.5 ([OS4], Prop 3.2). *For an equivalence class $U^m \otimes K$ of U -depth 0, there is a unique representative $(0, K)$ satisfying*

$$v_i \cdot v_i + 2 \leq K \cdot v_i \leq -v_i \cdot v_i \quad \text{for each vertex } v_i. \quad (3.1)$$

Conversely if a vector K satisfies (3.1), then K has U -depth 0 if and only if K supports a good full path (in this case K will be called a basic vector).

In the above, full path stands for a path of vectors K_1, K_2, \dots, K_n in $\text{Char}(G)$ with K_1 satisfying (3.1) obtained by adding $2PD[v_i]$ if $K_i \cdot v_j + v_j \cdot v_j = 0$ for some j , until $-K_n$ satisfies (3.1) or $K_n \cdot v_j + v_j \cdot v_j > 0$ for some j . It is called *good* if $-K_n$ satisfies (3.1).

In the proof of [OS4], Proposition 3.2, it is shown that given a characteristic vector M , the final vector of any full path is identical, hence we observe the following useful

Remark 3.6. Observe that if a vector supports a good full path, then all full paths are good, hence finding one bad full path means the initial vector is not basic. Secondly observe that bad full paths are hereditary, hence if a vector for a subgraph has a bad full path, then so does the containing vector and graph.

This will reduce the number of vectors that we need to check if they support a good full path or not. We will express the vectors $K \in \text{Char}(G)$ as sequences $(K \cdot v_i)$.

Lemma 3.7. *For the linear graph A_s with s vertices and each weight -2 , there are no good full paths starting at vectors K satisfying (3.1) with $K \cdot v_i = 2$ for more than one i .*

Proof. We will use induction on s , observing that we can use hereditary property of bad full paths. (3.1) implies $K \cdot v_i \in \{0, 2\}$. For $s = 2$, $(2, 2)$ for A_2 has a bad full

First we need to find characteristic vectors K satisfying inequality (3.1). There are only finitely many such vectors since G is a definite graph, in particular there are 80 characteristic vectors satisfying (3.1) for the given graph. Proposition 3.2 in [OS4] characterizes a spanning set for $K^+(G)$ which is the dual point of view for $H^+(G)$. Among the 80 characteristic vectors satisfying (3.1) we look for those vectors K which carry full paths ending at vectors L for which $-L$ satisfies (3.1). There are precisely three such vectors K and we list them and also the full paths for convenience (paths are obtained by consecutively adding $2PD(v_i)$ for the numbers i listed):

$$\begin{aligned} K_1 &= 12v_1 + 6v_2 + 3v_3 + 4v_4 + 2v_5 & \text{path: } 1,2,1 \\ K_2 &= -8v_1 - 4v_2 - v_3 - 2v_4 - 2v_5 & \text{path: } 1,2,1,5,4,1,2,1,3,1,2,1,4,1,2,1,5 \\ K_3 &= -16v_1 - 8v_2 - 3v_3 - 4v_4 - 2v_5 & \text{path: } 1,2,1 \end{aligned}$$

All other equivalence classes in $K^+(G)$ can be obtained using the U -action from these vectors. We must check which are distinct. From now on, we will write the vectors as 5-tuples with entries $\langle K, [v_i] \rangle$, hence K_i will be denoted as

$$(1, 0, -3, -2, 0), (1, 0, -3, -2, 2), \text{ and } (1, 0, -1, -2, 0).$$

The following diagram shows how $U \otimes K_1$, $U \otimes K_2$ and $U \otimes K_3$ are equivalent to $(-3, 4, 1, 2, 0)$, and hence to each other:

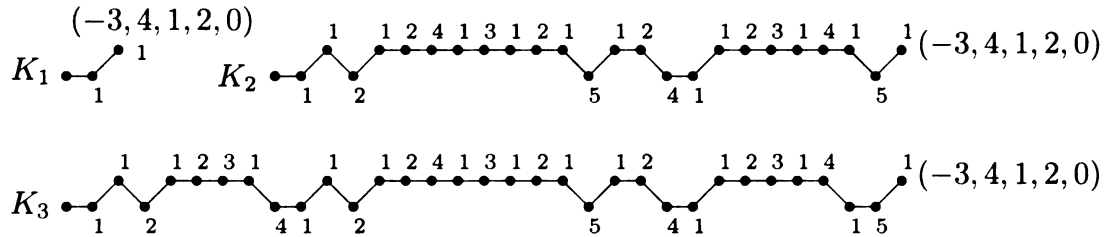


Figure 3.3: Equivalences in $K^+(G)$

In the above figure, vertices correspond to characteristic vectors and an edge ending with a number i means $2PD(v_i)$ was added to previous vector to reach the new one.

Edges with positive slope mean tensoring with U . Hence first diagram represents the vectors $(1, 0, -3, -2, 0), (-1, 2, -1, 0, 0), (-3, 4, 1, 2, 0)$ which tells us that

$$(1, 0, -3, -2, 0) \sim (-1, 2, -1, 0, 0) \text{ and } U \otimes (-1, 2, -1, 0, 0) \sim (-3, 4, 1, 2, 0)$$

Hence each K_i lies on the same grading level and we can check this by calculating

$$\frac{1}{4}(K \cdot K + |G|)$$

which is zero for each K_i . Therefore we conclude: $HF^+(-Y(G)) \cong T_0^+ \oplus \mathbb{Z}_{(0)} \oplus \mathbb{Z}_{(0)}$.

By Prop 7.11 of [OS2] we can convert this to the Heegard-Floer homology of $Y(G)$:

$$HF_*^+(Y(G)) = HF_-^{*-2}(-Y(G)) = T_0^+ \oplus \mathbb{Z}_{(-1)} \oplus \mathbb{Z}_{(-1)}$$

To do this, we first use the following long exact sequence to compute $HF^-(-Y(G))$:

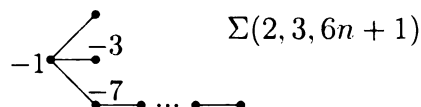
$$\dots \rightarrow HF^-(-Y(G)) \longrightarrow HF^\infty(-Y(G)) \longrightarrow HF^+(-Y(G)) \rightarrow \dots$$

then we adjust gradings by changing the signs and subtracting -2 . Note that here we adapted the convention of [OS4] by denoting $T_s^+ = \bigoplus_{k=0}^{\infty} \mathbb{Z}_{(s+2k)}$. So we have:

$$HF^+(\Sigma(2, 5, 7)) = T_0^+ \oplus \mathbb{Z}_{(-1)} \oplus \mathbb{Z}_{(-1)}$$

3.5 The family $\Sigma(2, 3, 6n + 1)$

Consider the family of Brieskorn spheres $Y(n) = \Sigma(2, 3, 6n + 1)$. The negative definite plumbing graph defining $Y(n)$ is a tree with weights -1 on central node, $-2, -3, -7$ on adjacent nodes and a -2 chain of length $n - 1$ starting at -7 as follows:



The Heegaard-Floer homology of the first member of this family, $HF^+(-\Sigma(2, 3, 7))$, has been studied in [OS4], [Ru1].

Lemma 3.8. *For arbitrary n , the basic vectors for $Y(n) = \Sigma(2, 3, 6n + 1)$ are*

$$\begin{aligned}
K_1 &= (1, 0, -1, -5, 0, 0, 0, \dots, 0) \\
K_2 &= (1, 0, -1, -3, 0, 0, 0, \dots, 0) \\
K_3 &= (1, 0, -1, -5, 2, 0, 0, \dots, 0) \\
K_4 &= (1, 0, -1, -5, 0, 2, 0, \dots, 0) \\
K_5 &= (1, 0, -1, -5, 0, 0, 2, \dots, 0) \\
&\vdots \\
K_{n+1} &= (1, 0, -1, -5, 0, 0, 0, \dots, 2)
\end{aligned}$$

Proof. Clearly for each j , K_j satisfies (3.1). Next we need to see that among all characteristic vectors satisfying (3.1) these are the only ones supporting good full paths. For $n = 1$ this is done in [OS4], and we verified it by computer.

By remark 3.6, for $n > 1$ first 4 entries of a basic vector has to coincide with one of $(1, 0, -1, -3)$, $(1, 0, -1, -5)$ which were computed in [OS4] for $n = 1$. Other entries are either 0 or 2. Moreover lemma 3.7 implies that for basic vectors K for $Y(n)$ there can be at most one vertex with $K \cdot v_i = 2$.

Claim. $(1, 0, -1, -3, *)$ has a bad path if $*$ has a non-zero entry.

Proof of claim. As in lemma 3.7, we can find a vector $(1, 0, -1, -3, 2, *)'$ equivalent to K . But $(1, 0, -1, -3, 2)$ has a bad path obtained by adding $2PD(v_i)$ in the order $i = 1, 2, 1, 3, 1, 2, 1, 5, 4, 1, 2, 1$ and bad paths are hereditary. \square

Hence the only basic vector with initial segment $(1, 0, -1, -3)$ is $(1, 0, -1, -3, 0, \dots, 0)$.

Next we need to show that K_1, \dots, K_{n+1} support good paths. This we do by explicitly giving the paths. First, $1, 2, 1, 3, 1, 2, 1$ is a good full path for both K_1 and K_2 . For others, the path starts the same, but continues as:

$$\begin{aligned}
& 5, 6, 7, \dots, n+3 \quad \text{for } K_3 \\
& 6, 5, 7, 6, 8, 7, \dots, n+3, n+2 \quad \text{for } K_4 \\
& 7, 6, 5, 8, 7, 6, 9, 8, 7, \dots, n+3, n+2, n+1 \quad \text{for } K_5 \\
& \vdots \\
& n+3, n+2, n+1, \dots, 5 \quad \text{for } K_{n+1}
\end{aligned}$$

This finishes the proof of the lemma. \square

For each K_i , when we compute the renormalized lengths $\frac{K \cdot K + |G|}{4}$, each time we get 0. Next we investigate relationships between U powers of K_i .

Lemma 3.9. $U \otimes K_i \sim U \otimes K_j \sim L = (-3, 2, 5, 1, 0, 0, \dots, 0)$ for $1 \leq i, j \leq n+1$

Proof. For K_1 , the sequence $1, 1, 2, 1$ leads to L .

For $i > 1$, the path from K_i leading to L is of the following form:

$$1, 1, 2, 1, 2, 3, 1, A_{n,i}, B_n$$

where B_n is $1, 2, 3, 1, 4, 1, 2, 1$ followed by $5, 6, \dots, n+3$ followed by 1 and $A_{n,i}$ is of the following form:

$$C_{n-i+1}, C_{n-i+2}, \dots, C_0.$$

In the above, C_k denotes the sequence $1, 2, 3, 1, 4, 1, 2, 1, 3, 1, 2, 1, 5, 6, 4+k$ if $k > 0$ and empty path if $k = 0$. As an example, for $n = 4$, the path from K_2 to L is given

by

$$\begin{aligned}
1, 1, 2, 1, 2, 3, 1, A_{4,2}, B_4 &= 1, 1, 2, 1, 2, 3, 1, C_3, C_2, C_1, B_4 \\
&= 1, 1, 2, 1, 2, 3, 1, \\
&\quad 1, 2, 3, 1, 4, 1, 1, 2, 1, 2, 3, 1, \\
&\quad 1, 2, 3, 1, 4, 1, 2, 1, 3, 1, 2, 1, 5, \\
&\quad 1, 2, 3, 1, 4, 1, 2, 1, 3, 1, 2, 1, 5, 6, \\
&\quad 1, 2, 3, 1, 4, 1, 2, 1, 5, 6, 7, 1
\end{aligned}$$

It is straightforward to check that these paths end at L . Next, one observes that as in [AD], throughout these paths the U -depth stays between 0 and 1, hence we get $U \otimes K_i \sim L$ as announced. \square

Proof of Theorem 3.2. Now we know that $K^+(G)$ consists of $U^0 \otimes K_1, U^0 \otimes K_2$ and $U^m \otimes K_1$ for $m > 0$. For any f in $\mathbb{H}^+(G)$, $f(K_1) \in T_0^+$ determines the images $\tilde{f}(m, K_1)$ of the induced map $\tilde{f} : \mathbb{Z} \times \text{Char}(G) \rightarrow T_0^+$. The remaining values $f(K_i)$ for $i > 1$ are also determined up to addition of an element of $\mathbb{Z}_{(0)}$. This finishes the proof of the theorem. \square

Note that Ozsváth and Szabó have computed HF^+ of this family with opposite orientation using a different method. After orientation reversal we see that the two computations agree.

Chapter 4

Invariants of cobordisms

4.1 d -invariant

Using absolute gradings, for rational homology 3-spheres Ozsváth and Szabó have defined [OS3] an invariant of $spin^c$ rational homology cobordism as follows:

Definition 4.1. Given a rational homology sphere (Y, t) , $d(Y, t)$ is the least absolute grading of the elements in $HF^+(Y, t)$ that lie in the image of $HF^\infty(Y, t)$ under the map induced by the projection π .

Theorem 4.2 ([OS3], Theorem 1.2). *d is an invariant of $spin^c$ rational homology cobordism between rational homology 3-spheres endowed with $spin^c$ structures.*

Since there is only one $spin^c$ structure on an integral homology sphere, if it bounds a rational homology 4-ball, it is rational homology cobordant to S^3 , hence we have

Corollary 4.3. *If an integral homology 3-sphere Σ bounds a smooth rational homology 4-ball, then $d(\Sigma) = 0$.*

In [AK], Akbulut and Kirby [AK] have shown $\Sigma(2, 5, 7)$, $\Sigma(3, 4, 5)$ and $\Sigma(2, 3, 13)$ bound contractible 4-manifolds. Also Casson and Harer [CH] and Stern [St] have

shown families of Seifert fibered homology spheres that bound contractible 4-manifolds. Since then some more sporadic examples have been shown. More recently Lisca has identified connected sums of lens spaces that bound rational homology balls.

The Neumann-Siebenmann invariant $\bar{\mu}$ gives another obstruction for Seifert fibered homology spheres to be homology cobordant to S^3 , which was proven by Saveliev [Sa3]. Also the invariant $R(\alpha_1, \dots, \alpha_n)$ defined by Fintushel and Stern [FS2] tells the central node in a minimal negative definite plumbing diagram has to be -1 if a Seifert fibered homology sphere bounds a \mathbb{Z}_2 -acyclic 4-manifold.

Remark 4.4. Fintushel and Stern [FS1] have shown that $\Sigma(2, 3, 7)$ bounds a rational homology 4-ball via constructing a rational homology cobordism using Kirby calculus. For this example $\bar{\mu} = 1$ whereas $d = 0$. Since $\bar{\mu} \neq 0$, $\Sigma(2, 3, 7)$ doesn't bound an integral homology 4-ball.

Given a negative definite plumbing diagram with at most one bad vertex, Ozsváth and Szabó [OS4] show that $d(Y, t)$ can be computed as the minimum of

$$-\frac{1}{4}(K \cdot K + |G|)$$

over all characteristic vectors K corresponding to the $spin^c$ structure t , where $|G|$ stands for the number of vertices in the plumbing graph G . This minimum is achieved among basic vectors, and using hereditary property we can reduce the number of characteristic vectors to check. This way we computed the values of d for the first few Brieskorn homology spheres. We present these data together with values of $\bar{\mu}$ in Table 4.1.

There are 79 Brieskorn homology spheres $\Sigma(p, q, r)$ with $0 < p < q < r \leq 13$. In Table 4.2 in page 32, we provide a list of those with $d = 0$. In Appendix pages 35–39 we provide the corresponding plumbing graphs.

Also we investigated the intersection forms of the canonical negative definite 4-manifolds $X(p, q, r)$ bounding the Brieskorn spheres given as the plumbed D^2 bundles over S^2 . Donaldson's theorem tells that the intersection form of a negative definite closed smooth 4-manifold X is diagonalizable over the integers, i.e., there is an integral matrix B with $B \cdot Q_X \cdot B^T = \pm Id$. This gives an obstruction for a homology sphere to bound a rational homology ball, in terms of intersection forms of negative definite fillings. We applied this to our particular examples:

Theorem 4.5. *Among all Brieskorn homology spheres $\Sigma(p, q, r)$ with $d = 0$ and $r < 13$, the intersection form of $X(p, q, r)$ is diagonalizable over the integers.*

Proof. The proof is given by explicitly constructing the matrices $B(p, q, r)$. At the time being we didn't obtain matrices B for $(7, 8, 9)$ and $(9, 10, 11)$, but since they fall into the category CH1, the intersection forms are diagonalizable over the integers. We provide a couple of examples below to give a taste of the process to the reader. The following denote the row-column operations to diagonalize the intersection form.

$\Sigma(3, 5, 8)$

$$\begin{array}{ll} 2 & \longrightarrow 2 + 1 \\ 4 & \longrightarrow 4 + 1 \\ 5 & \longrightarrow 5 + 1 \\ 3 & \longrightarrow 3 + 2 \\ 4 & \longrightarrow 4 + 2 \\ 5 & \longrightarrow 5 + 2 \\ 4 & \longrightarrow 4 + 3 \\ 5 & \longrightarrow 5 + 3 \\ 5 & \longrightarrow 5 + 4 \\ 4 & \longrightarrow 4 + 5 \end{array}$$

$\Sigma(5, 7, 9)$

$$\begin{array}{ll} 2 & \longrightarrow 2 + 1 \\ 4 & \longrightarrow 4 + 1 \\ 6 & \longrightarrow 6 + 1 \\ 3 & \longrightarrow 3 + 2 \\ 4 & \longrightarrow 4 + 2 \\ 6 & \longrightarrow 6 + 2 \\ 5 & \longrightarrow 5 + 4 \\ 6 & \longrightarrow 6 + 4 \\ 3 & \longrightarrow 3 + 5 \\ 6 & \longrightarrow 6 + 3 \\ 3 & \longrightarrow 3 + 6 \\ 5 & \longrightarrow 5 - 3 \\ 4 & \longrightarrow 4 - 5 \end{array}$$

□

p	q	r	d	$\bar{\mu}$
2	3	5	2	-1
3	4	5	0	0
2	3	7	0	1
2	5	7	0	0
3	4	7	2	-1
3	5	7	2	0
4	5	7	0	1
5	6	7	0	0
3	5	8	0	0
3	7	8	0	0
5	7	8	2	-1
2	5	9	2	-1
2	7	9	2	0
4	5	9	2	-1
4	7	9	4	-2
5	7	9	0	0
5	8	9	0	0
7	8	9	0	0
3	7	10	2	0
7	9	10	0	1
2	3	11	2	0
2	5	11	0	1
2	7	11	2	-1
2	9	11	0	0
3	4	11	2	-1
3	5	11	2	0
3	7	11	0	0
3	8	11	2	0
3	10	11	0	0
4	5	11	0	0
4	7	11	2	0
4	9	11	0	1
5	6	11	2	-1
5	7	11	2	-1
5	8	11	0	1
5	9	11	4	0
6	7	11	0	0
7	8	11	2	-1
7	9	11	2	0
7	10	11	2	-1
8	9	11	2	0
9	10	11	0	0

Table 4.1: Values of d and $\bar{\mu}$ for $r \leq 11$

p	q	r	comments
3	4	5	AK, CH1
2	3	7	$\bar{\mu} = 1$
2	5	7	AK, CH2
4	5	7	$\bar{\mu} = 1$
5	6	7	CH1
3	5	8	
3	7	8	CH1
5	7	9	
5	8	9	CH1
7	8	9	CH1
7	9	10	$\bar{\mu} = 1$
2	5	11	$\bar{\mu} = 1$
2	9	11	CH2
3	7	11	
3	10	11	CH1
4	5	11	
4	9	11	$\bar{\mu} = 1$
5	8	11	$\bar{\mu} = 1$
6	7	11	
9	10	11	CH1
5	7	12	$\bar{\mu} = 2$
5	11	12	CH1
7	11	12	$\bar{\mu} = 1$
2	3	13	AK, St, Fu
2	9	13	$\bar{\mu} = 1$
3	4	13	$\bar{\mu} = 1$
3	8	13	$\bar{\mu} = 1$
3	10	13	
4	11	13	CH2
5	6	13	$\bar{\mu} = 1$
5	11	13	
7	8	13	$\bar{\mu} = 1$
7	11	13	
7	12	13	CH1
8	11	13	
9	10	13	$\bar{\mu} = 1$
9	11	13	
10	11	13	
11	12	13	CH1

Table 4.2: List of Brieskorn spheres with $d = 0$ with $r \leq 13$

Chapter 5

Action of diffeomorphisms

5.1 An involution

In this section we show how Saveliev's theorem ([Sal], Theorem 15) translates into Heegaard Floer homology.

Theorem 5.1. *Let W^4 be a contractible manifold whose double is S^4 , and $Y = \partial W$ be a homology sphere with non-trivial \widehat{HF} . Then the involution $f : Y \# Y \rightarrow Y \# Y$ exchanging the summands acts non-trivially on $\widehat{HF}(Y \# Y)$.*

Proof. Consider the cobordism $X = (Y \times I) \natural W$, where \natural denotes boundary connected sum. This cobordism induces a homomorphism $F_X : \widehat{HF}(Y) \rightarrow \widehat{HF}(Y \# Y)$.

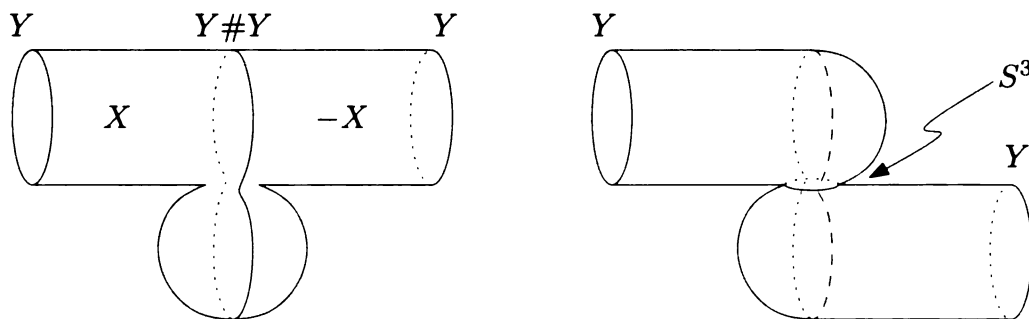


Figure 5.1: $Z_{id} = X \cup -X$ and $Z_f = X \cup_f -X$

Let $Z_{id} = X \cup_{Y \# Y} (-X)$ and $Z_f = X \cup_f (-X)$ (also compare to Matveyev [Mat] figure 2, page 576). Since $W \cup (-W) = S^4$, Z_{id} is diffeomorphic to the product $Y \times I$ relative to the boundary. By the functoriality of the induced maps, $F_{(-X)} \circ F_X = id : \widehat{HF}(Y) \longrightarrow \widehat{HF}(Y)$, hence F_X has to be injective.

Z_f is diffeomorphic to $X \cup_{Y \# Y} C_f \cup_{Y \# Y} (-X)$, where C_f is the mapping cylinder of the involution f . Again by functoriality, F_{Z_f} is the composition $F_{(-X)} \circ F_{C_f} \circ F_X$ and F_{Z_f} factors through $\widehat{HF}(S^3)$, as pictured in figure 5.1. Since we assume $\widehat{HF}(Y) \neq \mathbb{Z}$, we get $F_{C_f} \neq id$, hence the action induced by switching the summands acts non-trivially on $\widehat{HF}(Y \# Y)$. \square

Remark 5.2. The assumptions for the theorem are satisfied for several contractible 4-manifolds W . By results of Rustamov [Ru2], the only Brieskorn homology sphere with trivial \widehat{HF} is $\Sigma(2, 3, 5)$, which doesn't bound any contractible 4-manifold. Therefore any Mazur manifold W with Brieskorn homology sphere boundary gives an example that satisfies the assumptions.

This theorem also applies in the HF^+ setting:

Theorem 5.3. *Let W^4 be a contractible manifold whose double is S^4 , and $Y = \partial W$ be a homology sphere with non-trivial \widehat{HF} . Then the involution $f : Y \# Y \longrightarrow Y \# Y$ exchanging the summands acts non-trivially on $HF^+(Y \# Y)$.*

Appendix A

Plumbing graphs

Below we provide the plumbing graphs for the Brieskorn homology spheres $\Sigma(p, q, r)$ listed in Table 4.2, namely, those with $d = 0$ and $r \leq 13$. Vertices with no labels correspond to spheres of square -2 .



Table A.1: Plumbing graphs for $\Sigma(p, q, r)$ with $d = 0$ and $r \leq 13$

Table A.1 (cont'd)

$$\begin{array}{c} \bullet \\ \diagup \\ -1 \leftarrow \begin{array}{c} \bullet \\ -5 \\ \bullet \\ -8 \\ \bullet \end{array} \\ \diagdown \end{array} \quad \Sigma(3, 5, 8)$$

$$\begin{array}{c} \bullet \quad \bullet \quad \bullet \\ \diagup \\ \bullet \leftarrow \begin{array}{c} \bullet \\ -4 \\ \bullet \\ -3 \\ \bullet \end{array} \\ \diagdown \end{array} \quad \Sigma(5, 7, 8)$$

$$\begin{array}{c} \bullet \quad \bullet \\ \diagup \\ -1 \leftarrow \begin{array}{c} \bullet \\ -3 \\ \bullet \\ -4 \\ \bullet \\ -9 \end{array} \\ \diagdown \end{array} \quad \Sigma(5, 7, 9)$$

$$\begin{array}{c} \bullet \quad \bullet \\ \diagup \\ -1 \leftarrow \begin{array}{c} \bullet \\ -3 \\ \bullet \\ -3 \quad -3 \\ \bullet \\ -5 \end{array} \\ \diagdown \end{array} \quad \Sigma(5, 8, 9)$$

$$\begin{array}{c} \bullet \quad \bullet \\ \diagup \\ -1 \leftarrow \begin{array}{c} \bullet \\ -3 \\ \bullet \\ -8 \\ \bullet \\ -3 \end{array} \\ \diagdown \end{array} \quad \Sigma(7, 8, 9)$$

$$\begin{array}{c} \bullet \\ \diagup \\ -1 \leftarrow \begin{array}{c} \bullet \\ -7 \\ \bullet \\ -5 \\ \bullet \\ -4 \end{array} \\ \diagdown \end{array} \quad \Sigma(7, 9, 10)$$

$$\begin{array}{c} \bullet \\ \diagup \\ -1 \leftarrow \begin{array}{c} \bullet \\ -3 \\ \bullet \\ 11 \end{array} \\ \diagdown \end{array} \quad \Sigma(2, 5, 11)$$

$$\begin{array}{c} \bullet \\ \diagup \\ -1 \leftarrow \begin{array}{c} \bullet \\ -5 \\ \bullet \\ -4 \quad -3 \end{array} \\ \diagdown \end{array} \quad \Sigma(2, 9, 11)$$

$$\begin{array}{c} \bullet \\ \diagup \\ -1 \leftarrow \begin{array}{c} \bullet \\ -3 \\ \bullet \\ -4 \\ \bullet \\ 11 \end{array} \\ \diagdown \end{array} \quad \Sigma(3, 7, 11)$$

$$\begin{array}{c} \bullet \\ \diagup \\ -1 \leftarrow \begin{array}{c} \bullet \\ -3 \\ \bullet \\ -4 \\ \bullet \\ -3 \quad -4 \end{array} \\ \diagdown \end{array} \quad \Sigma(3, 10, 11)$$

Table A.1 (cont'd)

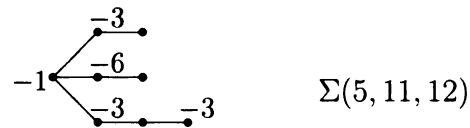
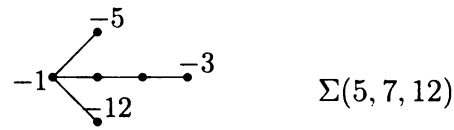
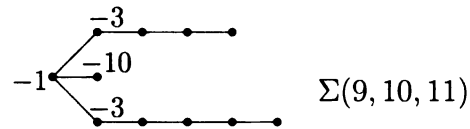
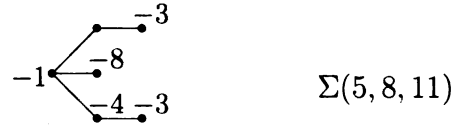
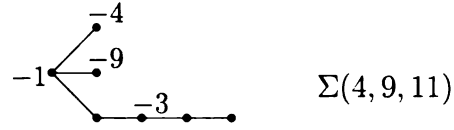
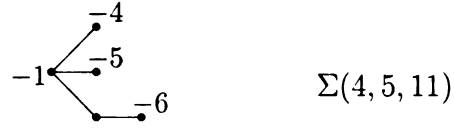


Table A.1 (cont'd)

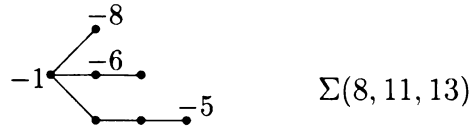
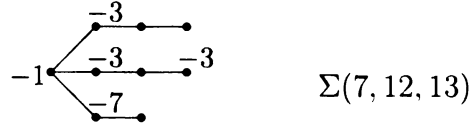
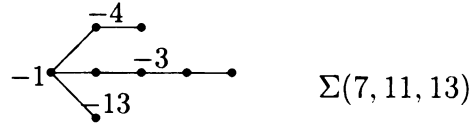
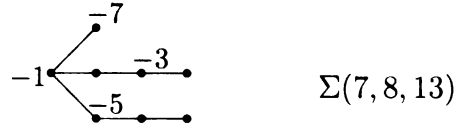
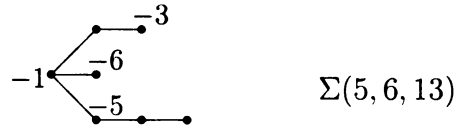
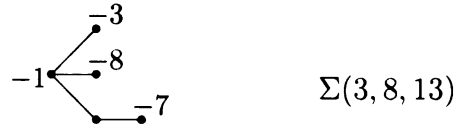
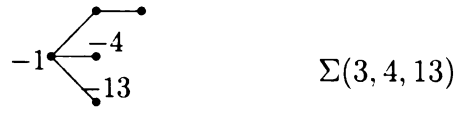
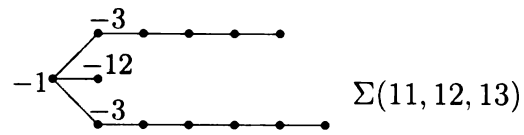
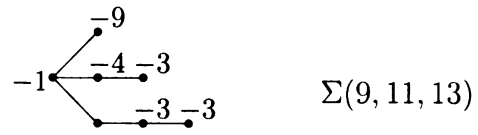
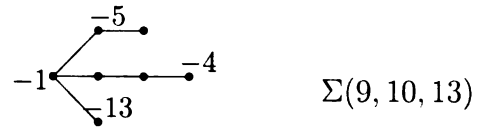


Table A.1 (cont'd)



Bibliography

- [AD] S. Akbulut, S. Durusoy, *An involution acting nontrivially on Heegaard-Floer homology*, in Geometry and topology of manifolds, Fields Inst. Commun., 47, 1–9, Amer. Math. Soc., Providence, RI, 2005
- [AK] S. Akbulut, R. Kirby, *Mazur manifolds*, Michigan Math. J. 26 (1979) 259–284
- [CH] A. Casson, J. Harer, *Some homology lens spaces which bound rational homology balls*, Pacific J. Math. 96 (1981), no. 1, 23–36
- [FS1] R. Fintushel, R. Stern, *A μ -invariant one homology 3-sphere that bounds an orientable rational ball*, Four-manifold theory (Durham, N.H., 1982), 265–268, Contemp. Math., 35, Amer. Math. Soc., Providence, RI, 1984.
- [FS2] _____, *Pseudofree orbifolds*, Ann. of Math. (2) 122 (1985), no. 2, 335–364
- [FS3] _____, *Instanton homology of Seifert fibred homology three spheres*, Proc. London Math. Soc. 61 (1990) 109–137
- [Fl1] A. Floer, *Morse theory for Lagrangian intersections*, J. Differential Geom. 28 (1988), no. 3, 513–547
- [Fl2] _____, *An instanton-invariant for 3-manifolds*, Comm. Math. Phys. 118 (1988), no. 2, 215–240
- [Li] P. Lisca, *Lens spaces, rational balls and the ribbon conjecture*, arXiv:math.GT/0701610
- [Mat] R. Matveyev, *A decomposition of smooth simply-connected h -cobordant 4-manifolds*, J. Differential Geom. 44 (1996), no. 3, 571–582
- [MO1] C. Manolescu, P. Ozsváth, S. Sarkar, *A combinatorial description of knot Floer homology*, arXiv:math/0607691
- [MO2] C. Manolescu, P. Ozsváth, Z. Szabó, D. Thurston, *Combinatorial link Floer homology*, arXiv:math/0610559
- [Ne] A. Némethi, *On the Ozsváth-Szabó invariant of negative definite plumbed 3-manifolds*, Geom. Topol. 9 (2005), 991–1042

- [OS1] P. Ozsváth and Z. Szabó, *Holomorphic disks and topological invariants for closed three-manifolds*, Ann. of Math. (2) 159 (2004), no. 3, 1027–1158
- [OS2] _____, *Holomorphic triangles and invariants for smooth four-manifolds*, Adv. Math. 202 (2006), no. 2, 326–400
- [OS3] _____, *Absolutely graded Floer homologies and intersection forms for four-manifolds with boundary*, Adv. Math. 173 (2003), no. 2, 179–261
- [OS4] _____, *On the Floer homology of plumbed three-manifolds*, Geom. Topol. 7 (2003) 185–224
- [Pe] T. Perutz, *A remark on Kähler forms on symmetric products of Riemann surfaces*, arXiv:math.SG/0501547
- [Ro] D. Rolfsen, *Knots and links*, Publish or Perish, 1976, reprinted by AMS 2003
- [Ru1] R. Rustamov, *Calculation of Heegaard Floer homology for a class of Brieskorn spheres*, arXiv:math.SG/0312071
- [Ru2] R. Rustamov, *On plumbed L-spaces*, arXiv:math.GT/0505349
- [SW] S. Sarkar, J. Wang, *An algorithm for computing some Heegaard Floer homologies*, arXiv:math/0607777
- [Sa1] N. Saveliev, *Floer homology and invariants of homology cobordism*, Internat. J. Math. 9 (1998), no. 7, 885–919
- [Sa2] _____, *An involution permuting Floer homology*, J. Knot Theory Ramifications 9 (2000), no. 4, 543–556
- [Sa3] _____, *Notes on homology cobordisms of plumbed homology 3-spheres*, Proc. Amer. Math. Soc. 126 (1998), no. 9, 2819–2825
- [St] R. Stern, *Some more Brieskorn spheres which bound contractible manifolds*, Notices Amer. Math. Soc. 25, A448. Abstract 78TG75

MICHIGAN STATE UNIVERSITY LIBRARIES



3 1293 02956 7918